Biosensors and Bioelectronics 26 (2011) 2864–2869

Contents lists available at ScienceDirect

Biosensors and Bioelectronics

journal homepage: www.elsevier.com/locate/bios

Ultra-sensitive biosensor based on mesocellular silica foam for organophosphorous pesticide detection

Shuo Wu[a,*], Lili Zhang[a], Lin Qi[b], Shengyang Tao[a], Xiaoqin Lan[a], Zhiguang Liu[a], Changgong Meng[a]

[a] School of Chemistry, Dalian University of Technology, Dalian 116023, PR China
[b] School of Materials Science and Engineering, Dalian University of Technology, Dalian 116023, PR China

ARTICLE INFO

Article history:
Received 16 August 2010
Received in revised form 2 November 2010
Accepted 19 November 2010
Available online 7 December 2010

Keywords:
Mesocellular silica foam
Solid phase extraction
Low limit of detection
Monocrotophos

ABSTRACT

A sensitive amperometric acetylcholinesterase (AChE) biosensor was fabricated based on mesocellular silica foam (MSF), which functioned as both an enzyme immobilization matrix and a solid phase extraction (SPE) material for the preconcentration of target molecules. The hydrophilic interface, the good mechanical/chemical stability, and the suitable pore dimension of MSF provided the entrapped AChE a good environment to well maintain its bioactivity at basic condition. The AChE immobilized in MSF showed improved catalytic ability for the hydrolysis of acetylthiocholine, as evidenced by the increasing of the oxidation current of thiocholine, the enzymatic catalytic hydrolysis production of acetylthiocholine. In addition, the MSF with large surface area showed a modest adsorption capacity for monocrotophos, a model organophosphate used in this study, *via* the hydrogen bond or physical adsorption interaction. The combination of the SPE and the good enzyme immobilization ability in MSF significantly promoted the sensitivity of the biosensor, and the limit of detection has lowered to 0.05 ng/mL. The biosensor exhibited accuracy, good reproducibility, and acceptable stability when used for garlic samples analysis. The strategy may provide a new method to fabricate highly sensitive biosensors for the detection of ultra-trace organophosphorous pesticide infield.

1. Introduction

Organophosphorous pesticides (OPs) are widely used in agriculture for pest control (Wang et al., 2008a; Lee et al., 2010). However, the toxic residuals of OPs in crop, livestock, and poultry products would cause the disfunction of neurotransmitter enzyme, acetylcholinesterase (AChE), and thus harm the human health (Mulchandani et al., 2001). The safety levels fixed by the national and international regulatory agencies depend on the toxicities of OPs, but the maximum concentration of each individual pesticide set by the European Council Directive 98/83/CE should be lower than 0.1 ppb, and the total amount must not exceed 0.5 ppb (Llopis et al., 2009). However, the low concentration of these compounds in food, water and air can hardly be monitored directly using standard analytical instrumentation. Gas chromatography (Noort et al., 2006) and high-performance liquid chromatography (Cappiello et al., 2002) coupled with mass spectroscopy could detect OPs in ppb level. Unfortunately, the tedious sample pretreatments, highly qualified technicians and sophisticated instruments are not suitable for infield detection. Consequently, the development of rapid and sensitive OPs detecting techniques with ultra-low detection limit shows increasing potential for environmental monitoring and food industry.

Amperometric AChE biosensors (Amine et al., 2006; Du et al., 2007; Hildebrandta et al., 2008) present a promising alternative method to the traditional strategies because of their high sensitivity, fast response, and miniature size. Based on the inhibition action of OPs on AChE, the concentration of pesticides could be precisely determined (Amine et al., 2006). The sensitivity and the detection limit of these biosensors depend on enzyme activity (Gong et al., 2009; Sotiropoulou and Chaniotakis, 2005), thus, the immobilization of enzyme on the surface of electrode is a crucial step for the performance of the biosensors. For the protection of enzyme activity, functional nanomaterials such as carbon nanotube (Kandimalla and Ju, 2006; Choi et al., 2009; Chen et al., 2008), gold nanoparticle (Du et al., 2007; Zhao et al., 2009), and mesoporous materials (Shimomura et al., 2009; Sotiropoulou and Chaniotakis, 2005) have been introduced for the construction of enzyme loaded matrix. The integration of advanced materials greatly promoted the sensitivity, stability and detection limit of AChE biosensors. Among them, the mesoporous materials have attracted considerable attention due to their large surface areas, versatile mesostructure, good mechanical/chemical stabilities (Wu et al., 2007; Dai et al., 2004). The pore diameter of mesoporous materials can be easily controlled between in a wide range (2–50 nm) to match the dimension of the immobilized enzyme. The nanopores provide confined space for enzymes

* Corresponding author. Tel.: +86 411 84706293.
E-mail address: wushuo@dlut.edu.cn (S. Wu).

0956-5663/$ – see front matter © 2010 Elsevier B.V. All rights reserved.
doi:10.1016/j.bios.2010.11.029

to prevent them from unfolding and are therefore beneficial for their activity maintenance (Zhou and Dill, 2001). The good enzyme activity maintenance ability of mesoporous materials has been well established by theoretical simulation (Zhou and Dill, 2001) and a large amount of experimental facts (Vamvakaki and Chaniotakis, 2007; Wu et al., 2007; Dai et al., 2004).

Mesoporous materials have been recently utilized for solid-phase extraction (SPE), which is applied in various fields, including separation science (Pérez-Quintanilla et al., 2007), on-line preconcentration and trace analysis (Trammell et al., 2008). In the past decades, this technique arose for the development of amperometric pesticides biosensors based on the principle of concentrating target pesticide on the surface of electrode, which significantly improve the sensitivity of the biosensors. Large surface area and adsorbing ability are required for a suitable SPE material. Compared with other SPE materials such as ZrO_2 nanoparticle (Du et al., 2008a), ZrO_2/Au nanocomposites film (Wang and Li, 2008), and multiwalled carbon nanotube (Du et al., 2008b), mesoporous material such as three dimensional mesocellular silica foam (MSF) is not only benefit from their large surface area, but pesticides compounds can interact with mesoporous silica with both physical adsorption and hydrogen bond. However, to the best of our knowledge, mesoporous materials are now barely used in the amperometric sensing of electro-inactive compounds for their SPE function. This is a blank area but with great perspective.

Herein, motivated by the super abilities of mesoporous materials, MSF was introduced to the surface of electrode for both enzyme immobilization and SPE of pesticides. An AChE biosensor was fabricated for the detection of a model OP, monocrotophos. The linear range was from 0.05 ppb to 10 ppb with a limit of detection down to 0.05 ppb, which satisfies the demand for ultra-trace pesticide detection.

2. Experimental

2.1. Reagents

Acetylcholinesterase (1000 U/mg) and acetylthiocholine chloride (ATCl) were purchased from Sigma–Aldrich (St Louis, USA) and used as received. Monocrotophos was purchased from Treechem Co. (Shanghai, China). Poly(vinyl alcohol) (PVA) and poly(ethylene oxide)-block-poly-(propylene)-block-poly(ethylene oxide) ($EO_{20}PO_{70}EO_{20}$, Pluronic P123) was purchased from BASF (Germany). 5,5′-Dithiobis(2-nitrobenzoic acid) was purchased from Boao Co. (Shanghai, China). All other reagents were of analytical grade and used without further purification. 0.1 M phosphate buffer solution (PBS) was prepared by mixing the stock solutions of NaH_2PO_4 and Na_2HPO_4. Doubly distilled water was used in all experiments.

2.2. Preparation of AChE loaded MSF suspension

MSF powder was synthesized according to the method reported previously (Schmidt-Winkel et al., 2000). 0.5 mg of the obtained MSF powder was first mixed with 1.0 mL water and stirred for 2 h to obtain the MSF suspension. Then 17 U AChE was added into the suspension and shaken for 20 min to obtain the enzyme entrapped MSF nanocomposite.

2.3. Construction of AChE-MSF-PVA/GCE

Glassy carbon electrodes (3 mm in diameter, CH Instruments, Inc., U.S.A.) were firstly polished to a mirror finish with 0.3 and 0.05 μm alumina slurry followed by thoroughly rinsing with deionized water. After sonicating successively in 1:1 nitric acid, acetone and deionized water, the electrodes were rinsed with deionized water and dried at room temperature. Then 3 μL of the AChE loaded MSF suspension and 3 μL 2% PVA aqueous solution was subsequently cast on the GCE to obtain the AChE-MSF-PVA/GCE, with the total AChE amount of 50 mU on the electrode surface. The PVA membrane could fix the AChE impregnated MSF nanocomposite on electrode surface. The biosensor was stored at 4 °C when not in use. For comparison, AChE-PVA/GCE, MSF-PVA/GCE, and PVA/GCE were fabricated.

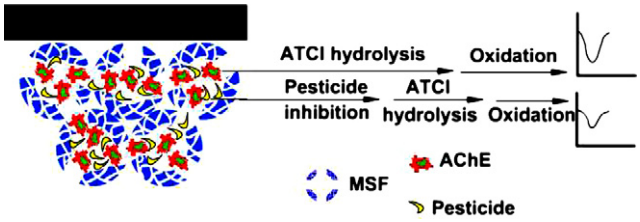

Fig. 1. Schematic diagram for biosensor fabrication and determination of monocrotophos.

2.4. Inhibition measurement using AChE biosensor

A detailed description of the assay process for monocrotophos was illustrated in Fig. 1. For inhibition tests, the original differential pulse voltammetric signal ($I_{P,control}$) was measured in 0.1 M pH 9.0 PBS with 1.5 mM ATCl. Then the electrode was rinsed with water and incubated in an aqueous solution containing the desired concentration of monocrotophos for 10 min. After incubation, the residual signal ($I_{P,exp}$) was recorded at the same condition. The inhibition rate of monocrotophos was calculated as follows:

$$\text{Inhibition}\,(\%) = 100\% \times \frac{I_{P,control} - I_{P,exp}}{I_{P,control}}$$

2.5. Activity and stability assays

500 mg MSF powders were added into 10 mL AChE solution (activity of 20 U), and the mixture was shaken at room temperature in a shaken bath for 2 h for the adsorption of enzyme in the MSF. Then the AChE/MSF composite was centrifuged and washed with deionized water twice. No enzyme was detected in the supernatant according to the Ellman method (Ellman et al., 1961). The composite was dried at 30 °C and stored at −20 °C. The amount of immobilized enzyme in the porous MSF was calculated as 40 mU/mg.

In order to measure the stability of the immobilized enzyme, the AChE/MSF composite was dispersed in pH 9.0 PBS (10 mg/mL). Aliquots were taken every 20 min over a time period of 120 min from the AChE/MSF suspension to analyze its activity using a modified Ellman method (Ellman et al., 1961). For comparison, the stability of the free enzyme in pH 9.0 PBS was also examined.

2.6. Adsorption of monocrotophos

The AChE-MSF-PVA/GCE or the AChE-PVA/GCE was immersed in 1.0 mL 500 ppb monocrotophos solution for 10 min for monocrotophos adsorption. The residual monocrotophos amount after adsorption was calculated by UV adsorption at 265 nm.

2.7. Apparatus

The electrochemical measurements were carried out on a CHI 660c electrochemical working station (CH Instruments Co.). A three-electrode system was employed with AChE-MSF-PVA/GCE as working electrode, a saturated calomel electrode (SCE) as reference

electrode and a platinum wire as counter electrode. Transmission electron microscopy (TEM) experiments were performed on a JEM-300CX electron microscope (JEOL, Japan) with an acceleration voltage of 300 kV. The nitrogen adsorption/desorption isotherms and pore size distribution (calculated by the Barrett-Joyner-Halenda model) were measured at 77 K using a Micrometeritics ASAP 2020 system. The UV–vis spectra were measured by a UV-1201 spectrometer (Ruili, Beijing, China).

3. Results and discussion

3.1. Morphology and pore size distribution of MSF

The TEM image of MSF showed uniformly distributed mesocells with diameter of about 29 nm (Fig. S1), indicating a typical mesocellular structure. Fig. S2A shows the N_2 adsorption/desorption isotherms of MSF, which exhibited large hysteresis with sharp adsorption and desorption branches at high relative pressure, indicating the narrow pore size distribution of large mesopores (Wu et al., 2007). From the adsorption and desorption branches of the isotherms the pore size distribution can be calculated using the Barrett–Joyner–Halenda method, which was shown in Fig. S2B. Obviously, the MSF displayed two main kinds of mesopores centered at 12.5 and 28.5 nm, respectively, indicating the MSF was composed of main cells with a diameter of 28.5 nm interconnected by 12.5 nm windows. The window diameter of 12.5 nm matched well with the dimensions of AChE molecule (7.0 nm × 10 nm × 12 nm) (Raves et al., 1998), which facilitated the entrance of AChE into the mesopores. The 28.5 nm diameter of the main cell was about 2–3 times larger than the dimension of AChE, the value just satisfied the demand for protein immobilization and bioactivity maintenance, which has been proven by both theoretical calculations (Zhou and Dill, 2001) and the experimental result that the AChE maintained 102% of its activity after being immobilized in the mesopores. The slight improvement of AChE activity was attributed to the configuration change of the enzyme inside the confined space. The Brunaur–Emmett–Teller surface area and mesopore volume of the MSF were calculated to be 460 m^2/g and 2.09 cm^3/g, respectively, which could separately accommodate more enzymes and concentrate pesticide therein.

3.2. UV–vis spectra

To evaluate the adsorption of monocrotophos on MSF, UV–vis spectrometry was introduced for the investigation. UV–vis spectra of monocrotophos solution before (curve a) and after SPE on AChE-PVA/GCE (curve b) and AChE-MSF-PVA/GCE (curve c) were shown in Fig. 2. The freshly prepared monocrotophos (500 ppb) exhibited an obvious absorption peak centered at 265 nm (curve a), which was the characteristic absorbance peak of monocrotophos. After 10 min adsorbed on the AChE-MSF-PVA/GCE, the adsorption peak (curve c) intensity obviously decreased, indicating a significant decrease of the monocrotophos amount in the solution. The monocrotophos adsorption amount on the AChE-MSF-PVA/GCE was about 3 times larger than that of AChE-PVA/GCE (curve b). The excellent adsorption ability of the MSF to monocrotophos may because the MSF has a large surface area and abundant amount of silanols thus could bind with monocrotophos *via* nonspecific adsorb or hydrogen bond interaction. We assume the adsorption on the adhesive PVA could be attributed to the high oxygen content of PVA, which might form hydrogen bonds with the monocrotophos. The special ability of the mesopores to adsorb monocrotophos could increase the local concentration of pesticide around the AChE, which in turn contributed to the improvement of the sensitivity, and allowed for the detection of pesticide with ultra-low concentration.

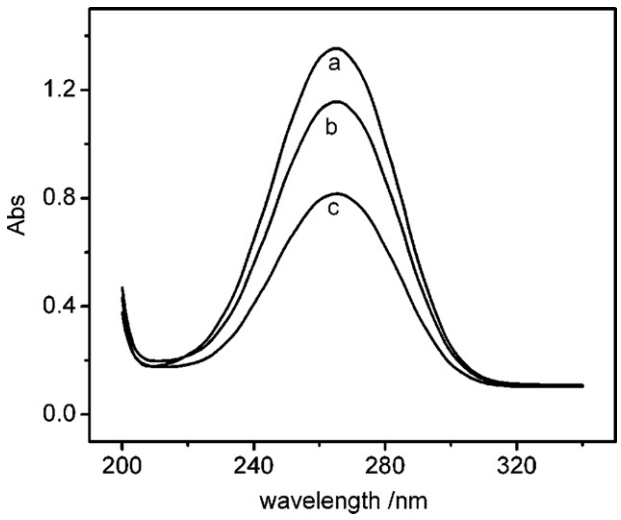

Fig. 2. Uv–vis spectra of 0.5 μg/mL monocrotophos solution before (a) and after SPE by AChE-MSF-PVA/GCE (b), and AChE-PVA/GCE (c) for 10 min.

3.3. Cyclic voltammetry behavior of the biosensor

Fig. 3A shows the cyclic voltammograms (CVs) of different electrodes in pH 9.0 PBS containing 1.5 mM ATCl. No detectable signal was observed at the PVA/GCE and the MSF-PVA/GCE without immobilization of AChE (curve a and curve b), which showed that both PVA and MSF were electroinactive in the potential window. The CV of the AChE-MSF-PVA/GCE showed an irreversible oxidation peak at 680 mV (curve d), which resulting from the oxidation of thiocholine, hydrolysis product of ATCl, catalyzed by the enzyme. In contrast, without the addition of MSF, the peak current of the AChE-PVA/GCE was much lower (curve c). The increase of the response may due to the fact that the MSF with large surface area and suitable pore size could immobilize more amount of enzymes and well maintain the maximum bioactivity of the immobilized enzyme.

After 10 min incubation in 5 ng/mL and 10 ng/mL monocrotophos solution, the anodic peak currents (curves b and c, Fig. 3B) dramatically decreased compared with the control (curve a, Fig. 3B), and the decrease in peak current increased with the increasing concentration of monocrotophos. This was because monocrotophos as one of the OP compounds exhibited acute toxicity and involved in the irreversible inhibition action on AChE, thus reduced the enzymatic activity to its substrate. Based on the change in voltammetric signal of the AChE-MSF-PVA/GCE, the monocrotophos concentration could be detected.

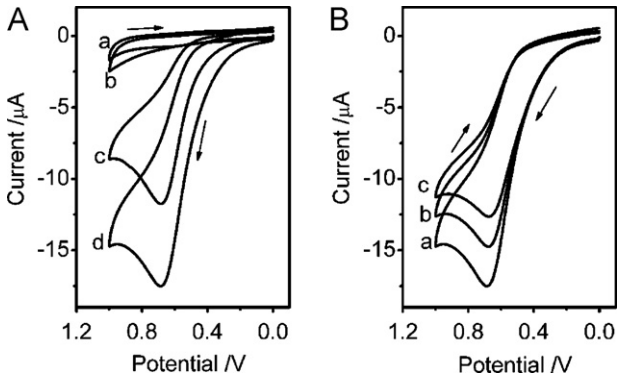

Fig. 3. (A) CVs of the PVA/GCE (a), MSF-PVA/GCE (b), AChE-PVA/GCE (c), and AChE-MSF-PVA/GCE (d) in 0.1 M PBS 9.0 solution containing 1.5 mM ATCl, and (B) CVs of AChE-MSF-PVA/GCE in PBS 9.0 solution before (a) and after the inhibition by 5 ng/mL(b) and 10 ng/mL (c) monocrotophos. Scan rate 50 mV/s.

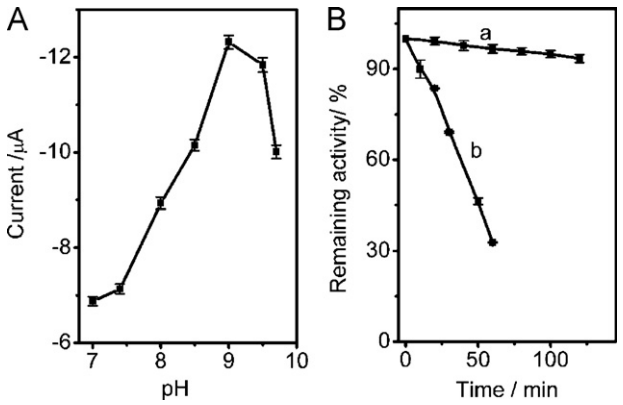

Fig. 4. (A) Influence of pH value on the response of the AChE-MSF-PVA/GCE to 1.5 mM ATCl at 0.7 V. (B) Stability of the MSF entrapped (a) and the free AChE (b) in pH 9.0 PBS solutions.

With increasing the scan rate, the peak current increased and the peak potential shifted slightly (Fig. S3). The peak currents exhibited a linear dependence on the scan rates ranging from 20 to 200 mV/s, indicating a typical surface-controlled electrode process. On the contrary, if the enzyme was in aqueous solution, a diffusion-controlled process could be observed and the peak currents would exhibit a linear dependence on the square root of scan rate. So, our results indicated that AChE was firmly immobilized in MSF with little leaching during the detection process. This may be due to the strong interaction between the silica wall of MSF and the enzyme as well as the physical entrapment effect of the small pore entrances (windows).

3.4. Calibration curve of ATCl

Fig. S4 shows the amperometric response of the AChE-MSF-PVA/GCE to the addition of ATCl. The typical current–time response curve of the biosensor was obtained by successive additions of the substrate into a stirred cell. With the increasing concentration of ATCl the amperometric response increased, and got to a plateau at 1.5 mM, indicating a typical Michealis–Menten process. And the 1.5 mM ATCl was therefore chosen as the uniform concentration in the following experiments for the pesticides analysis. The apparent Michaelis–Menten constant (K_m^{app}) was estimated to be 0.38 mM according to the Lineweaver–Burk equation (inset B in Fig. S4). The value was lower than those of 0.45 mM for AChE adsorbed on AuNPs–SiSG composite film (Du et al., 2007), and 1.5 mM for AChE adsorbed on polyethyleneimine modified electrode (Joshi et al., 2005). Thus, the immobilized AChE on MSF matrix exhibited a higher affinity to ATCl. The high affinity of the enzyme may lie in two aspects. On one hand, the confined space in the mesopores would prevent the immobilized enzyme from unfolding, thus well maintain the activity of the enzyme. On the other hand, the hydrophilic surface is beneficial for the AChE to take the orientation of active center upward due to the repulsion between the hydrophobic active gorge and the hydrophilic interface therefore facilitate the contact of the enzyme and its substrates (Zhao et al., 2009).

3.5. Influence of pH value

For the electrochemical biosensors, the pH value was a crucial factor influencing the sensitivity and stability. Therefore, we further investigated the effect of pH. As shown in Fig. 4A, the maximum amperometric response of the AChE-MSF-PVA/GCE to 1.5 mM ATCl was obtained at pH = 9.0, different from most of the reported AChE biosensors that exhibited the maximum amperometric response

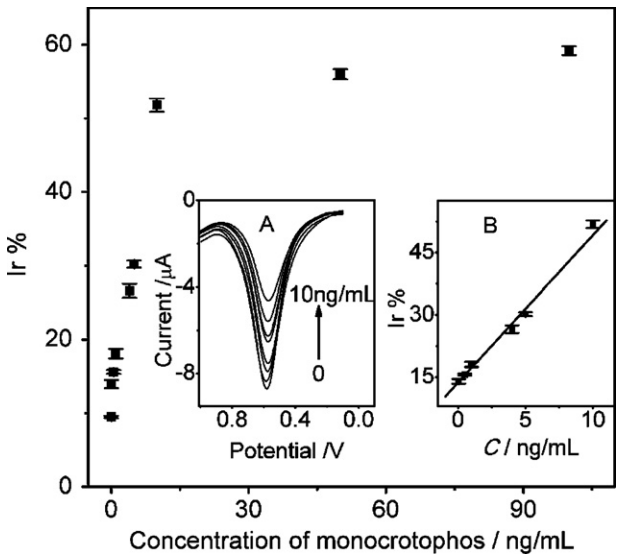

Fig. 5. Inhibition curve of the biosensor with different monocrotophos concentrations. (From lower to higher, the inhibitions were corresponding to the monocrotophos of 0.005, 0.05, 0.5, 1, 4, 5, 10, 50, and 100 ng/mL, respectively.) Inset, DPV curves (A) and calibration curve for monocrotophos determination (B).

at neutral conditions (Kandimalla and Ju, 2006; Du et al., 2007). It is well-known that the effect of pH on the AChE based biosensor lies in two aspects, the activity of the immobilized enzymes and the enzymatic reaction (Zhao et al., 2009). On one hand, basic condition facilitates the oxidation of thiocholine, by generating H^+ and RSSR (Wang et al., 2008b). Thus the response of the proposed biosensor would increase with the increase of pH. On the other hand, extreme pH conditions would result in the denaturization of enzyme. These results proved that the MSF could effectively protect the enzyme from denaturation at basic conditions, up to pH 9.0. The good ability of the MSF in protecting the enzyme under basic condition (pH 9.0) has been confirmed, as shown in Fig. 4B. The AChE entrapped in the MSF had well maintained its activity, after 60 min treatment in pH 9.0 PBS, its activity still remained 96.7%. In contrast, without the protection of the MSF, the activity of the free enzyme sharply decreased and only 32.8% of the activity was survived. We attributed this to the robust framework and unique pore structure of MSF which provided the entrapped enzymes a confined space and thus prevented them from denaturing even under relatively extreme conditions.

3.6. Application of AChE-inhibition biosensors: detection of monocrotophos

One of the most influencing parameters in pesticide analysis was the incubation time for the inhibition. With increasing incubation period the percentage of the inhibition also increased. The incubation time required for the inhibition was checked at different time intervals from 3 to 60 min (Fig. S5). With an increasing incubation time the inhibition increased and reached the maximum value after the incubation time of 10 min in 10 ng/mL monocrotophos solution. Thus, 10 min was used for the assay. Under the optimal conditions, the inhibition was proportional to the monocrotophos concentration ranging from 0.05 to 10 ng/mL (Fig. 5), with the detection limit of 0.05 ng/mL. The performance of this AChE-MSF-PVA/GCE compared with other reported AChE biosensors was summarized in Table 1. It shows that the present AChE-MSF-PVA/GCE exhibited comparable or lower limit of detection, indicating that MSF with multifunctions in enzyme immobilization, enzyme activity maintenance, and SPE could contribute a lot to the sensitivity enhancement.

Table 1
The key parameters of AChE biosensors for pesticide detection.

Method	Pesticide detected	Linear range	Limit of detection	References
AChE-AuNP–polypyrrole nanowires	Methyl parathion	0.005–0.12 ppm 0.5–4.5 ppm	2 ppb	Gong et al. (2009)
Au–TiO_2/chitosan	Parathion	1.0 ppb–7.0 ppm	0.5 ppb	Qu et al. (2008)
AChE-(*x*GnPs)–chitosan		0.005–0.039 μM	0.158 nM	Ion et al. (2010)
AuNPs-MWCNTs–chitosan microspheres–AChE	Monocrotophos	0.1–10 μM	10 nM	Norouzi et al. (2010)
AChE/Al_2O_3/sonogel	Paraoxon Dichlorvos Chlorpyrifos-ethyl-oxon		7.5 nM 0.5 nM 0.25 nM	Zejli et al. (2008)
MWNT-AChE/PB/MWNT biosensor	Dichlorvos/carbofuran:		0.04 ppb/0.1 ppb	
nano$CaCO_3$/chitosan/AChE	Methyl parathion	0.005–0.2 ppm 0.75–3.75 ppm	1 ppb	Gong et al. (2009)
AChE/gold nanoparticle/sol–gel	Monocrotophos	0.001–1 ppm 2–15 ppm	0.6 ppb	Du et al. (2007)
CdTe/gold nanoparticles modified chitosan microspheres	Monocrotophos	1–1000 ppb 2–15 ppm	0.3 ppb	Du et al. (2008c)
MWCNT for solid-phase extraction	Methyl parathion	0.05–2.0 ppm	5 ppb	Du et al. (2008b)
AChE/MWNT	Dichlorvos/carbofuran		0.04 ppb/0.1 ppb	Chen et al. (2008)
AChE biosensor coupled with a preconcentration and oxidation on a solid phase column.	Paraoxon/dichlorvos		25 nM/25 nM	Dondoi et al. (2006)
AChE/MWNT	Paraoxon		0.7 nM	Wang et al. (2008a,b)
AChE-MSF-PVA	Monocrotophos	0.05–10 ppb	0.05 ppb (0.2 nM)	Our method

3.7. Precision of measurements and stability of biosensor

The inter-assay precision was estimated at five different electrodes for the determinations in 1.5 mM ATCl after being treated with 5 ng/mL monocrotophos solutions for 10 min. The R.S.D. of inter-assay was found to be 6.2%, indicating acceptable precision and reproducibility. When the enzyme electrode was not in use, it was stored at 4 °C in dry condition. No obvious decrease in the response of ATCl was observed in the first 7-day storage. After a 30-day storage period, the sensor retained 92% of its initial current response.

3.8. Reactivity and real sample analysis

The reactivation of AChE was another important factor influencing the biosensor performance. AChE, which has been irreversibly inhibited by OPs, could be completely reactivated by using nucleophilic compounds such as pralidoxime chloride (PAM-Cl). PAM-Cl PBS solution with concentration of 5.0 mM was used for the reactivation. After the biosensor has been used for monocrotophos inhibition, it was immersed in the PAM-Cl solution. After regeneration for 10 min, the activity of the AChE has been totally regenerated. With the reactivation procedure this biosensor could be repeatedly used for 6 cycles with an acceptable reproducibility.

To further demonstrate the practicality of the proposed biosensor, the recovery test was studied by adding different amounts of monocrotophos into garlic samples. Results were summarized in Table S1. The recoveries were from 90.8% to 110%. The results indicated that the proposed method was highly accurate, precise and reproducible. It could be used for direct analysis of relevant samples.

4. Conclusion

In this paper, a sensitive and stable biosensor has been constructed based on the AChE entrapped MSF, which enabled the detection of ultra-trace (0.05 ng/mL) organophosphorous compound monocrotophos. The use of MSF has significantly improved the performance of the biosensor in three aspects: (1) the large pore volume and suitable pore dimension allowed the immobilization of enzymes without aggregation; (2) the suitable pore/window dimensions and good mechanical/chemical stability rendered MSF the ability to well maintain the AChE activity against high basic condition, thus promoted the enzymatic reaction process; (3) MSF acted as a SPE material to concentrate organophosphorous compounds in the mesopores thus improving the local concentration of pesticide therein. Owing to these three important enhancement factors, the resulted biosensor showed extremely high sensitivity and low limit of detection, and was therefore more suitable for ultra-trace detection of OP pesticides residue compared with other AChE biosensors.

Acknowledgements

The authors gratefully acknowledge the financial support of the National Natural Science Foundation of China (Nos. 20805003, 20903018), the Research Fund for the Doctoral Program of Higher Education of China (No. 200801411106), and the Young Teachers' Training Foundation (893383) of Dalian University.

Appendix A. Supplementary data

Supplementary data associated with this article can be found, in the online version, at doi:10.1016/j.bios.2010.11.029.

References

Amine, A., Mohammadi, H., Bourais, I., Palleschi, G., 2006. Biosensors Bioelectronics 21, 1405–1423.
Cappiello, A., Famiglini, G., Palma, P., Mangani, F., 2002. Analytical Chemistry 74, 3547–3554.
Chen, H.D., Zuo, X.L., Su, S., Tang, Z., Wu, A., Song, S.P., Zhang, D.B., Fan, C.H., 2008. Analyst 133, 1182–1186.
Choi, B.G., Park, H., Park, T.J., Kim, D.H., Lee, S.Y., Hong, W.H., 2009. Electrochemistry Communications 11, 672–675.
Dai, Z.H., Liu, S.Q., Ju, H.X., Chen, H.Y., 2004. Biosensors Bioelectronics 19, 861–867.
Du, D., Chen, S.Z., Cai, J., Zhang, A.D., 2007. Biosensors Bioelectronics 23, 130–134.
Du, D., Ye, X.P., Zhang, J.D., Zeng, Y., Tu, H.Y., Zhang, A.D., Liu, D.L., 2008a. Electrochemistry Communications 10, 686–690.
Du, D., Wang, M.H., Zhang, J.M., 2008b. Electrochemistry Communications 10, 85–89.
Du, D., Chen, S.Z., Song, D.D., Li, H.B., Chen, X., 2008c. Biosensors Bioelectronics 24, 475–479.
Dondoi, M.P., Bucur, B., Danet, A.F., Toader, C.N., Barthelmebs, L., Marty, J.L., 2006. Analytica Chimica Acta 578, 162–169.
Ellman, G.L., Courtney Jr., K.D., Andres, V., Featherstone, R.M., 1961. Biochemical Pharmacology 7, 88–95.

Gong, J.M., Wang, L.Y., Zhang, L.Z., 2009. Biosensors Bioelectronics 24, 2285–2288.
Hildebrandta, A., Bragósb, R., Lacortea, S., Marty, J.L., 2008. Sensors and Actuators B 133, 195–201.
Ion, A.C., Ion, I., Culetu, A., Gherase, D., Moldovan, C.A., Iosub, R., Dinescu, A., 2010. Materials Science and Engineering C 30, 817–821.
Joshi, P.P., Merchant, S.A., Wang, Y.D., Schmidtke, D.W., 2005. Analytical Chemistry 77, 3183–3188.
Lee, J.H., Park, J.Y., Min, K., Cha, H.J., Choi, S.S., Yoo, Y.J., 2010. Biosensors Bioelectronics 25, 1566–1570.
Kandimalla, V.B., Ju, H.X., 2006. Chemistry A: European Journal 12, 1074–1080.
Llopis, X., Pumera, M., Alegret, S., Merkoc, A., 2009. Lab on a Chip 9, 213–218.
Mulchandani, A., Chen, W., Mulchandani, P., Wang, J., 2001. Biosensors Bioelectronics 16, 225–230.
Noort, D., Fidder, A., van der Schans, M.J., Hulst, A.G., 2006. Analytical Chemistry 78, 6640–6644.
Norouzi, P., Pirali-Hamedani, M., Ganjali, M.R., Faridbod, F., 2010. Journal of Electrochemistry Science 5, 1434–1446.
Pérez-Quintanilla, D., Sánchez, A., Hierro, I.d., Fajardo, M., Sierra, I., 2007. Journal of Separation Science 30, 1556–1567.
Qu, Y.H., Min, H., Wei, Y.Y., Xiao, F., Shi, G.Y., Li, X.H., Jin, L.T., 2008. Talanta 76, 758–762.
Raves, M.L., Giles, K., Schrag, J.D., 1998. Structure and Function of Cholinesterases and Related Proteins. Plenum Publishing, New York, p. 351–356.
Schmidt-Winkel, P., Lukens, W.W., Yang, P.D., 2000. Chemistry of Materials 12, 686–696.
Shimomura, T., Itoh, T., Sumiya, T., Mizukami, F., Ono, M., 2009. Enzyme and Microbial Technology 45, 443–448.
Sotiropoulou, S., Chaniotakis, N.A., 2005. Analytica Chimica Acta 530, 199–204.
Trammell, S.A., Zeinali, M., Melde, B.J., Charles, P.T., Velez, F.L., Dinderman, M.A., Kusterbeck, A., Markowitz, M.A., 2008. Analytical Chemistry 80, 4627–4633.
Vamvakaki, V., Chaniotakis, N.A., 2007. Biosensors Bioelectronics 22, 2650–2655.
Wang, H., Wang, J., Timchalk, C., Lin, Y.H., 2008a. Analytical Chemistry 80, 8477–8484.
Wang, J., Timchalk, C., Lin, Y.H., 2008b. Environmental Science Technology 42, 2688–2693.
Wang, M., Li, Z.Y., 2008. Sensors and Actuators B 133, 607–612.
Wu, S., Ju, H.X., Liu, Y., 2007. Advanced Functional Materials 17, 585–592.
Zejli, H., Hidalgo-Hidalgo de Cisneros, J.L., Naranjo-Rodriguez, I., Liu, B.H., Temsamani, K.R., Marty, J.L., 2008. Talanta 77, 217–221.
Zhao, W., Ge, P.Y., Xu, J.J., Chen, H.Y., 2009. Environmental Science Technology 43, 6724–6729.
Zhou, H.X., Dill, K.A., 2001. Biochemistry 40, 11289–11293.